Atmos. Chem. Phys. Discuss., 10, 1983–2003, 2010
www.atmos-chem-phys-discuss.net/10/1983/2010/

Atmospheric Chemistry and Physics Discussions

This discussion paper is/has been under review for the journal Atmospheric Chemistry and Physics (ACP). Please refer to the corresponding final paper in ACP if available.

Estimating the maritime component of aerosol optical depth and its dependency on surface wind speed using MODIS and QuikSCAT data

Y. Lehahn[1,2], I. Koren[2], E. Boss[3], Y. Ben-Ami[2], and O. Altaratz[2]

[1]Department of Geophysics and Planetary Sciences, Tel Aviv University, Tel Aviv, Israel
[2]Department of Environmental Sciences, Weizmann Institue, Rehovot, Israel
[3]School of Marine Sciences, University of Maine, Orono, Maine, USA

Received: 12 December 2009 – Accepted: 21 January 2010 – Published: 29 January 2010

Correspondence to: Y. Lehahn (yoav.lehahn@weizmann.ac.il)

Published by Copernicus Publications on behalf of the European Geosciences Union.

Abstract

Seven years (2002–2008) of satellite measurements from SeaWinds aboard Quick Scatterometer (QuikSCAT) and Moderate Resolution Imaging Spectroradiometer (MODIS) aboard Terra are used for providing a global view on the link between surface wind speed and marine aerosol optical depth. This study shows that away form the continents the correlation time between the surface winds and the marine aerosol exceeds 4 h and therefore the two measurements can be linked. A systematic comparison between the satellite derived fields at different locations over the World Ocean allows to: (i) separate the relative contribution of wind-induced marine aerosol to the aerosol optical depth (ii) identify a threshold wind speed for triggering maritime contribution to aerosol optical depth; and (iii) extract an empirical linear equation linking marine aerosol optical depth and wind intensity. Wind induced marine aerosol contribution to aerosol optical depth is found to be dominated by the coarse mode elements. The threshold wind speed for triggering emission of coarse maritime aerosol is remarkably consistent with an average value of 4.1±0.1 m/s. When wind intensity exceeds the threshold value, coarse mode marine aerosol optical depth is linearly correlated to the surface wind speed, with a consistent slope of 0.0082±0.0004 s/m. The background aerosol optical depth, associated with aerosols that are not produced in-situ through wind driven processes, shows relatively large seasonal and geographical variability, and can be used for estimating the contribution of terrestrial aerosols to the aerosol optical depth over the ocean.

1 Introduction

Covering approximately 70% of the Earth's surface, the World Ocean is one of the major sources of natural aerosol. Marine aerosols play an important role in altering Earth's energy balance, either through direct scattering of solar radiation or indirectly through altering cloud microphysical properties, and therefore are important constituents of the

ACPD
10, 1983–2003, 2010

climate system and of the hydrological cycle. Changes in marine aerosol properties are likely to have important climatological implications (Kaufman et al., 2002; Murphy et al., 1998; Latham and Smith, 1990; Charlson et al., 1992).

Marine aerosols comprise two components: (i) primary aerosols, which are generated at the sea surface through wind driven processes (especially the bursting of entrained air bubbles associated with whitecap formation) resulting in mechanical production of sea-spray particles and (ii) secondary aerosols, which are the outcome of gas-to-particle processes (O'Dowd and de Leeuw, 2007). Sea spray aerosol contribute to both fine and coarse aerosol modes, with dominant fractions of inorganic sea salt and organic matter in the supermicron and submicron modes, respectively (Cavalli et al., 2004). It is well established that the generation of sea spray aerosols (Nilsson et al., 2001), as well as the consequent particle concentration (Hoppel et al., 1990; Glantz et al., 2004; O'Dowd et al., 1997) and size distribution (Hoppel et al., 1990; Gong et al., 1997) are strongly dependent on the wind speed.

Thus, correct representation of marine aerosol characteristics and their dependency on surface wind speed are essential for climate forcing estimations and accurate modeling of the climate system. Currently, our understanding of these phenomena is limited by the availability of observational data. Measurements of aerosol parameters such as aerosol optical depth (τ), fraction of coarse aerosol (f_c) and the relative contribution to τ by fine (τ_f) and coarse (τ_c) particles from the Moderate Resolution Imaging Spectroradiometer (MODIS) (Remer et al., 2008), in conjunction with satellite measurements of the surface wind speed (W), provide the means for continuous, long term global observations of this complex system.

A major obstacle for making a comprehensive use of satellite data for quantifying phenomena associated with marine aerosols stems from the fact that the majority of the oceans cannot be considered pristine, as they show evidence of aerosol loading from terrestrial origin (Huang et al., 2009). Overall, aerosols over the ocean can be classified into three main groups: marine aerosol, anthropogenic aerosol (biomass burning and pollution) and dust. Accordingly, satellite measurements of aerosol optical depth are the sum of contributions from all aerosol groups:

$$\tau = \tau_a + \tau_d + \tau_m \tag{1}$$

Where the subscripts a, d, and m denote anthropogenic, dust, and marine aerosol components, respectively. Currently, our ability to distinguish between the different types of aerosols is limited. Given that the fraction of fine particles in anthropogenic aerosol is much higher as compared to dust or maritime aerosol (Kaufman et al., 2002), a limited classification of aerosol type is possible by the spectral dependence that is linked to the aerosol size. Nevertheless, we do not have an efficient mechanism to distinguish between maritime aerosol and dust in the MODIS data (Kaufman et al., 2005b). In previous works, τ_m was determined empirically as a constant or as a function of near-surface wind speed from the National Center for Environmental Prediction (NCEP) (Kaufman et al., 2001, 2005a,b).

Here we suggest a novel approach to distinguish the maritime from other components of τ, based on a systematic comparison of satellite measurements of aerosol optical parameters and W. We show that satellite measured surface wind speed can serve as a reliable proxy for the spatial distribution of coarse marine aerosol. More specifically, this work is aimed at providing (i) a mechanism for identifying the maritime component of satellite derived τ and τ_c (τ_{cm}), and (ii) a global perspective on the dependency of τ_m and τ_{cm} on W.

Previous studies of the link between τ and W were carried out in specific locations over the world ocean, resulting in a variety of linear (Smirnov et al., 2003; Villevalde et al., 1994), power-law (Mulcahy et al., 2008; Glantz et al., 2009) and exponential (Moorthy and Satheesh, 2000; Vinoj and Satheesh, 2003) relationships between the fields. Exponential increase in aerosol optical depth with increasing wind speeds, were also found by Satheesh et al. (2006) who made use of τ from MODIS and W from NCEP over the Arabian Sea. More recently, Huang et al. (2009) studied the effect of wind speed on τ at 550 nm over remote pristine ocean regions using satellite estimates of τ from Advanced Along-Track Scanning Radiometer (AATSR) and wind speeds from the European Center for Medium-Range Weather Forecast (ECMWF). Their results from 3 pristine ocean regions show linear relationship between the fields.

The methodology and satellite datasets used in this research are described in the following section. The proposed mechanism for separating the maritime component of τ and τ_c and the results of the comparison between the fields are described in Sect. 3 followed by a summary and conclusions in Sect. 4.

2 Data and methods

Analysis of the link between aerosol parameters and surface wind speed is based on comparison between daily satellite measurements over a seven years period, from 2002 to 2008.

2.1 Satellite data

2.1.1 Aerosol properties

Aerosol parameters were derived from MODIS aboard NASAs satellite Terra that follows a sun-synchronous orbit, crossing the equator at approximately 10:30 LT. The dataset used here is from the Terra Collection005, consisting of daily global level 3 images (LAADS, http://ladsweb.nascom.nasa.gov/). The spatial resolution is 1°. MODIS aerosol optical parameters and aerosol size parameters are standard MODIS products and were found to be in good agreement with the same quantities derived by AERONET instruments on the ground (Remer et al., 2005, 2008).

2.1.2 Surface wind speed

Surface wind speeds were obtained from the SeaWinds scatterometer on board NASA's Quick Scatterometer (QuikSCAT) satellite (Freilich et al., 1994). The satellite's orbit, which is sun-synchronous, is optimized to measure winds over 90% of the

Earth at least once per day. The level 3 data that were used in this research are provided on an approximately 0.25°×0.25° global grid. Only data from ascending passes (06:00 LT equator crossing) were included. QuikSCAT data were obtained through the on line PO.DAAC Ocean ESIP Tool (POET) at the Physical Oceanography Distributed Active Archive Center (PO.DAAC), NASA Jet Propulsion Laboratory, Pasadena, CA (http://podaac.jpl.nasa.gov/poet).

2.2 Regions of interest

The comparison between wind speed and aerosol parameters was performed over 5 5×5° regions of interest (ROI) at different locations over the World Ocean (regions a–e in Fig. 1a). In order to minimize contribution from terrestrial sources, the ROIs were defined in areas that are (i) located away from known sources and transport routes of terrestrial aerosol and (ii) characterized by low mean τ and hence less affected by long-range aerosol transport. Another issue that was taken into consideration when choosing the ROIs is the 4.5 h time difference between the wind and aerosol measurements (06:00 LT for QuikSCAT measurements and 10:30 LT for MODIS-Terra measurements). Hence, the ROIs were defined in regions away from the coastline, where the wind regime is not effected by sea breeze (Gille et al., 2003). In these regions, within the 4.5 h time frame the correlation between W and τ_c is well kept. When increasing the time difference between the measurements to longer periods the correlation between the fields decreases significantly due to synoptic changes in the wind field (Fig. 2).

Based on these criteria, adequate areas were identified in the North and South Pacific (regions a,b centered respectively at 177.5° W/27.5° N and 147.5° W/27.5° S), North and South Atlantic (regions c,d centered respectively at 37.5° W/37.5° N and 17.5° W/27.5° S) and the Indian Ocean (region e, centered at 77.5° E/27.5° S).

2.3 Statistical analysis

For each ROI, time series of wind speed and aerosol parameters were extracted separately over 25 $1\times1^{\circ}$ cells (each cell covered by one pixel of MODIS data and 16 pixels of QuikSCAT data). In order to avoid extreme (and hence poorly represented) values, the highest 3% of the W and τ_c data were excluded. The data were sorted according to W and divided into 30 bins of equal number of observations. Regression equations and correlation coefficients were calculated from the full cloud of data points before binning. The statistical analysis was performed on the daily data, without spatial and temporal averaging.

2.4 Approach

In order to separate the maritime component of τ, we suggest a novel method that takes into account the additional (satellite derived) information on the surface wind speed. The approach we take is based on the assumption that, as a first approximation, the component of τ_c that correlates with W over the oceans is τ_{cm} (Satheesh et al., 2006). This assumption is supported by Kaufman et al. (2005b) analysis of vertical profiles of wind driven aerosol concentration over the Atlantic Ocean, that showed that the lowest 500 m of the atmosphere are mostly occupied by sea salt aerosol, whereas dust away from the source is transported at higher altitudes. The lack of correlation between W and the dust component of τ_c (τ_{cd}) is emphasized in Fig. 3, where we plot W and τ_c over a $5\times5^{\circ}$ region (region DD in Fig. 1a) in an area known to be dominated by desert dust offshore Africa (Kaufman et al., 2002). Regression analysis shows no significant correlation between W and τ_c in this area. Anthropogenic aerosols are predominately fine-mode (Kaufman et al., 2002) and are considered to have very little effect on τ_c (Satheesh et al., 2006).

ACPD
10, 1983–2003, 2010

2.5 Comparison with ground measurements

Correlating data from QuikSCAT and MODIS for studying wind-aerosol interactions over the ocean may be limited by the effect of reflection by whitecaps, which are also strongly linked to the wind speed and might bias aerosol retrieval (Yu et al., 2009). In order to evaluate the feasibility of the methodology, a comparison was made with data from the land-based AERONET station in Midway Island, where wind speed effects on marine aerosols optical properties were thoroughly investigated by Smirnov et al. (2003). AERONET data (level 1.5, ONEILL-15 – provisional status) for the years 2001–2008 were downloaded from the AERONET web-page (http://aeronet.gsfc.nasa.gov/). A daily sample was calculated as the mean of all measurements taken between 6 a.m. and 10 a.m. MODIS and QuikSCAT data were averaged daily over a $2\times2^{\circ}$ area around the station. The relationship between W and aerosol optical parameters (τ, τ_c and τ_f) from MODIS (Fig. 4, left panels) and from the AERONET station (Fig. 4, right panels) are similar. For moderate winds (W smaller than approximately 5 m/s) both MODIS and AERONET τ (Fig. 4a and b) and τ_c (Fig. 4c and d) are almost constant, with typical values of approximately 0.1 and 0.05, respectively. For stronger winds the two parameters increase linearly with W. τ_f from both MODIS and AERONET show little or no change over the whole range of wind speeds, with MODIS τ_f being slightly higher than that from AERONET.

3 Analysis and results

On an annual time scale W and f_c show similar distribution patterns over large parts of the World Ocean (Fig. 1). Note that the correlation are better over the open oceans away form the shores. Moreover, it is shown that areas of strong annual winds are characterized by large fraction of coarse mode aerosol and high values of τ_c (Fig. 1d). Regions of moderate winds are usually characterized by a relatively small fraction of coarse mode aerosol and low values of τ_c. A different picture is found in the Atlantic

ACPD
10, 1983–2003, 2010

Title Page
Abstract Introduction
Conclusions References
Tables Figures
◀◀ ▶▶
◀ ▶
Back Close
Full Screen / Esc
Printer-friendly Version
Interactive Discussion

Ocean east of Africa and in the Arabian Sea, where prominent features of high τ_c associated with dust (Kaufman et al., 2002) are found in regions of weak or intermediate W.

As can be seen in Fig. 5, the relationship between W and τ_c in the 5 ROIs can be divided into two phases associated with the wind intensity: (i) a "tranquil" phase where τ_c is nearly constant and (ii) a "windy" phase where τ_c is linearly correlated with W. Since, as suggested above, any correlation between W and τ_c actually reflects correlation with τ_{cm}, we can now identify a threshold wind speed (W_{thc}) for triggering contribution to τ_c from wind induced marine aerosols. W_{thc} is objectively defined as the highest value of W corresponding to τ_c equal or smaller than τ_c of the first bin (i.e. the strongest wind associated with the "tranquil" phase). In the 5 ROIs W_{thc} (red circle in Fig. 5) is remarkably consistent, with an average value of 4.1±0.1 m/s. When excluding data corresponding to winds below W_{thc}, the correlation coefficient R between τ_c and W range from 0.37 to 0.45 and are statistically significant at the 99% confidence level. The slope (α_c) linking τ_c to W is remarkably consistent, with an average value of 0.0082±0.0004 s/m.

Following that, we identify a background aerosol (τ_{c0}, marked by the horizontal line in Fig. 5), which is a measure to the contribution to τ_c from all aerosols not produced in situ through wind driven processes, by averaging τ_c associated with winds below W_{thc}. τ_{c0} varies between 0.03 to 0.05 with an average value of 0.04±0.01. Then, τ_{cm} is simply calculated as:

$$\tau_{cm} = \tau_{c0} + \alpha_c(W - W_{thc}) \tag{2}$$

Further investigation of the link between W and marine aerosol optical properties is done by plotting τ, τ_c and τ_f against W for all the data associated with the 5 ROIs (Fig. 6). The relationship between τ and W (Fig. 6a) is remarkably similar to the relationship between τ_c and W (Fig. 6b), with a threshold wind speed (W_{th}) of 3.8±0.2 m/s and a slope α of 0.011 ± 0.002 s/m. The background component of τ (τ_0) is twice higher than τ_{c0} (0.08).

Hence, equation in the form of Eq. (2), can be used for estimating the wind induced marine aerosol contribution to τ:

$$\tau_m = \tau_0 + \alpha(W - W_{th}) \tag{3}$$

The similarity between τ and τ_c relationships with W can be explained by the low correlation between W and τ_f (Fig. 6c). Since τ is simply the sum of τ_c and τ_f, and since τ_f shows little dependency on the wind speed, increase in τ due to wind driven emission of marine aerosols is attributed almost entirely to contribution from coarse mode particles. τ_f has an important contribution to the part of τ that is independent of the wind speed (i.e. the background aerosol), with a value 0.04 being about half of the total τ_0.

Seasonal and geographical variations in the parameters describing the relationships of τ and τ_c with W are examined in Fig. 7. The threshold wind speed for triggering contribution of maritime aerosols to τ and τ_c (Fig. 7a and b, respectively), show very little variability, maintaining a value of approximately 4 m/s throughout the year in all 5 ROIs. The slopes α and α_c linking W with τ_c and τ_c, respectively, have mean values of 0.011 ± 0.001 s/m and 0.0083 ± 0.0001 s/m, (Fig. 7c and d, respectively).

The parameters showing the largest spatio-temporal variability are τ_0, with values ranging from 0.05 to 0.17 and 0.18 (Fig. 7e) and τ_{c0}, with values ranging from 0.02 to 0.07 (Fig. 7f). The large geographical and seasonal variations in τ_0 and τ_{c0} are attributed to changes in the emission and transport of aerosol from terrestrial sources (Kaufman et al., 2002). Since the background aerosol optical depth is a measure to all aerosols not produced in situ through wind driven processes, regions characterized by low values of τ_0 (e.g. ROI e during the months June–August) and τ_{c0} (e.g. ROI d during the months December–February) can be considered as relatively pristine, with little contribution of aerosols from terrestrial sources.

Comparison with previous works (dashed lines in Fig. 6a), suggests that the power law relationship obtained by Mulcahy et al. (2008) can be used as a first approximation to the link between satellite derived surface wind speed and marine aerosol optical depth found here.

4 Summary and conclusions

Using a novel methodology based on a systematic comparison between satellite measurements of surface wind speed from QuikSCAT and aerosol parameters from MODIS, we conclude that:

1. At a given location over the open sea, instantaneous measurements within a few hours time frame are adequate for quantifying the link between wind and coarse marine aerosols.

2. Changes in aerosol optical depth due to wind induced maritime aerosols are dominated by contribution from coarse mode particles.

3. Similarly to the "threshold wind" for emission of desert dust (Chomette et al., 1999), there is a remarkably consistent threshold wind speed of 4.1 ± 0.1 m/s for triggering emission of coarse maritime aerosol allover our study area. This threshold value is strongly supported by the fact that 4 m/s is typically estimated as the wind speed at which whitecap formation onset occurs (O'Dowd and de Leeuw, 2007).

4. When surface wind speed exceeds the threshold value, coarse marine aerosol optical depth is linearly correlated to the surface wind speed, with a consistent slope of 0.0082 ± 0.0004 s/m.

5. Assuming that over the open sea, away from the continents, optical depth by other types of coarse particles (such as dust) is not well correlated with surface wind, having the wind information, the total aerosol optical depth and the fine fraction enables estimation of the marine aerosol contribution to the total coarse optical depth and therefore, to a good approximation, the contribution of coarse mode dust. Moreover, by deducting the wind induced marine aerosol, the average background aerosol loading can be estimated per location and season.

ACPD

10, 1983–2003, 2010

The satellite based analysis demonstrated here covers a large variety of oceanic and atmospheric regimes throughout a relatively long (7 years) time span, hence including a wide range of wind speeds and aerosol properties. The results from this analysis significantly improve our ability to distinguish between different aerosol types over the World Ocean and provide a framework for continuous, long term observations on the production of marine aerosols, and on the way they affect, and are affected by, climate variability.

Acknowledgements. We would like to acknowledge the partial support of the Minerva Foundation (grant 780048) and of Yeda-Sela center. The work of Y.L. was supported by the Dan David Prize Scholarship (2008).

References

Cavalli, F., Facchini, M., Decesari, S., Mircea, M., Emblico, L., Fuzzi, S., Ceburnis, D., Yoon, Y., O'Dowd, C., Putaud, J.-P., and Dell'Acqua, A.: Advances in characterization of size-resolved organic matter in marine aerosol over the North Atlantic, J. Geophys. Res., 109, D24215, doi:10.1029/2004JD005137, 2004. 1985

Charlson, R., Schwartz, S., Hales, J., Cess, R., Coakley, J., Hansen, J., and Hofmann, D.: Climate forcing by anthropogenic aerosols, Science, 255, 423–430, 1992. 1985

Chomette, O., Legrand, M., and Marticorena, B.: Determination of the wind speed threshold for the emission of desert dust using satellite remote sensing in the thermal infrared, J. Geophys. Res., 104, 31207–31215, 1999. 1993

Freilich, M., Long, D., and Spencer, M.: SeaWinds: A scanning scatterometer for ADEOS II – Science overview, in: Proc. Int. Geoscience and Remote Sensing Symp., IEEE, Pasadena, CA, 960–963, 1994. 1987

Gille, S., Smith, S., and Lee, S.: Measuring the sea breeze from QuikSCAT scatterometry, Geophys. Res. Lett., 30, 1114, doi:10.1029/2002GL016230, 2003. 1988

Glantz, P., Svensson, G., Noone, K., and Osborne, S.: Sea-salt aerosols over the North-east Atlantic: model-2 Second Lagrangian experiment, Q. J. Roy. Meteor. Soc., 130, 2191–2215, 2004. 1985

Glantz, P., Nilsson, E., and von Hoyningen-Huene, W.: Estimating a relationship between aerosol optical thickness and surface wind speed over the ocean, Atmos. Res., 92, 58–68, 2009. 1986

Gong, S., Barrie, L., and Blanchet, J.-P.: Modeling sea-salt aerosols in the atmosphere, 1. Model development, J. Geophys. Res., 102, 3805–3818, 1997. 1985

Hoppel, W., Fitzgerald, J., Frick, G., Larson, R., and Mack, E.: Aerosol size distributions and optical properties found in the marine boundary layer over the Atlantic Ocean, J. Geophys. Res., 95, 3659–3686, 1990. 1985

Huang, H., Thomas, G. E., and Grainger, R. G.: Relationship between wind speed and aerosol optical depth over remote ocean, Atmos. Chem. Phys. Discuss., 9, 24511–24529, 2009, http://www.atmos-chem-phys-discuss.net/9/24511/2009/. 1985, 1986, 2002

Kaufman, Y., Smirnov, A., Holben, B., and Dubovik, O.: Baseline maritime aerosol: methodology to derive the optical thickness and scattering properties, Geophys. Res. Lett., 17, 17, doi:10.1029/2001GL013312, 2001. 1986

Kaufman, Y., Tanré, D., and Boucher, O.: A satellite view of aerosols in the climate system, Nature, 419, 215–223, 2002. 1985, 1986, 1989, 1991, 1992

Kaufman, Y., Boucher, O., Tanré, D., Chin, M., Remer, L., and Takemura, T.: Aerosol anthropogenic component estimated from satellite data, Geophys. Res. Lett., 32, L17804, doi:10.1029/2005GL023125, 2005a. 1986

Kaufman, Y., Koren, I., Remer, L. A., Tanré, D., Ginoux, P., and Fan, S.: Dust transport and deposition observed from the Terra-Moderate Resolution Imaging Spectroradiometer (MODIS) spacecraft over the Atlantic Ocean, J. Geophys. Res., 110, D10S12, doi:10.1029/2003JD004436, 2005b. 1986, 1989

Latham, J. and Smith, M.: Effect on global warming of wind-dependent aerosol generation at the ocean surface, Nature, 347, 372–373, 1990. 1985

Moorthy, K. and Satheesh, S.: Characteristics of aerosols over a remote island, Minicoy in the Arabian Sea: optical properties and retrieved size characteristics, Q. J. Roy. Meteor. Soc., 126, 81–109, 2000. 1986

Mulcahy, J., O'Dowd, C., Jennings, S., and Ceburnis, D.: Significant enhancement of aerosol optical depth in marine air under high wind conditions, Geophys. Res. Lett., 35, L16810, doi:10.1029/2008GL034303, 2008. 1986, 1992, 2002

Murphy, D., Anderson, J., Quinn, P., McInnes, L., Brechtel, F., Kreidenweis, S., Middlebrook, A., Pósfai, M., Thomson, D., and Buseck, P.: Influence of sea-salt on aerosol radiative properties in the Southern Ocean marine boundary layer, Nature, 392, 62–65, 1998. 1985

Nilsson, E., Rannik, U., Swietlicцki, E., Leck, C., Aalto, P., Zhou, J., and Norman, M.: Turbulent aerosol fluxes over the Arctic Ocean: 2. Winddriven sources from the sea, J. Geophys. Res., 106, 32111–32124, 2001. 1985

O'Dowd, C. and de Leeuw, G.: Marine aerosol production: a review of the current knowledge, Philos. T. R. Soc. A, 365, doi:10.1098/rsta.2007.2043, 2007. 1985, 1993

O'Dowd, C., Smith, M., Consterdine, I., and Lowe, J.: Marine aerosol, sea-salt, and the marine sulphur cycle: a short review, Atmos. Environ., 31, 73–80, 1997. 1985

Remer, L., Kaufman, Y., Tanré, D., Mattoo, S., Chu, D., Martins, J., Li, R.-R., Ichoku, C., Levy, R., Kleidman, R., Eck, T., Vermote, E., and Holben, B.: The MODIS aerosol algorithm, products, and validation, J. Atmos. Sci., 947–971, 2005. 1987

Remer, L., Kleidman, R., Levy, R., Kaufman, Y., Tanré, D., Mattoo, S., Martins, J., Ichoku, C., Koren, I., Yu, H., and Holben, B.: Global aerosol climatology from the MODIS satellite sensors, J. Geophys. Res., D14S07, doi:10.1029/2007JD009661, 2008. 1985, 1987

Satheesh, S., Srinivasan, J., and Krishna Moorthy, K.: Contribution of sea-salt to aerosol optical depth over the Arabian Sea derived from MODIS observations, Geophys. Res. Lett., 33, L03809, doi:10.1029/2005GL024856, 2006. 1986, 1989

Smirnov, A., Holben, B., Eck, T., Dubovik, O., and Slutsker, I.: Effect of wind speed on columnar aerosol optical properties at Midway Island, J. Geophys. Res., 108, 4802, doi:10.1029/2003JD003879, 2003. 1986, 1990, 2002

Villevalde, Y., Smirnov, A., O'Neill, N., Smyshlyaev, S., and Yakovlev, V.: Measurement of aerosol optical depth in the Pacific Ocean and the North Atlantic, J. Geophys. Res., 99, 983–988, 1994. 1986

Vinoj, V. and Satheesh, S.: Measurements of aerosol optical depth over Arabian Sea during summer monsoon season, Geophys. Res. Lett., 30, 1263, doi:10.1029/2002GL016664, 2003. 1986

Yu, H., Chin, M., Remer, L., Kleidman, R., Bellouin, N., Bian, H., and Dieh, T.: Variability of marine aerosol fine-mode fraction and estimates of anthropogenic aerosol component over cloud-free oceans from the Moderate Resolution Imaging Spectroradiometer (MODIS), J. Geophys. Res., 114, D10206, doi:10.1029/2008JD010648, 2009. 1990

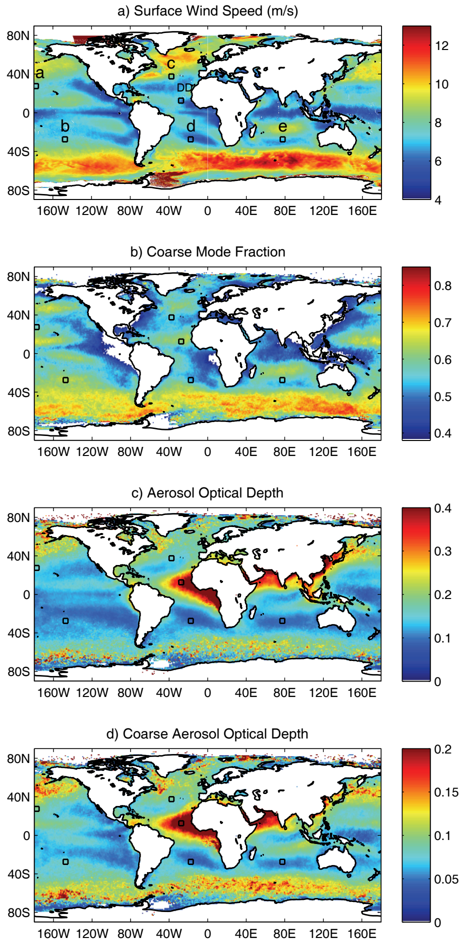

Fig. 1. 2004 annual mean distribution of **(a)** W; **(b)** f_c; **(c)** τ; **(d)** τ_c. The black boxes and the letters in panel (a) indicate regions used in the analysis presented in the following figures.

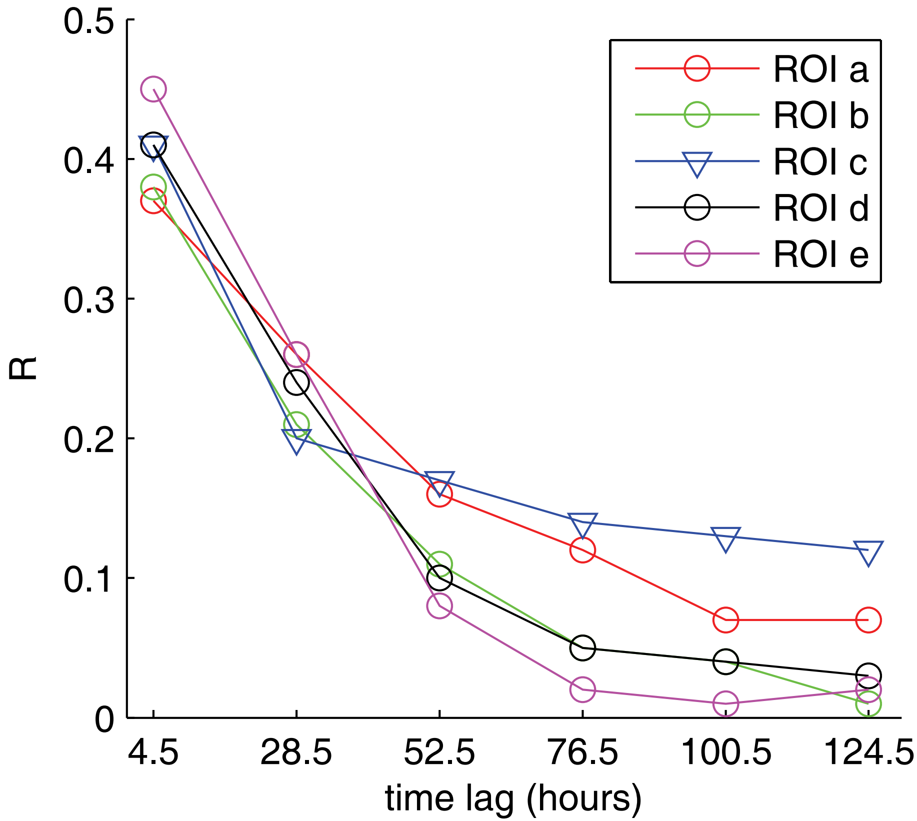

Fig. 2. Correlation coefficients between MODIS τ_c and QuikSCAT W as a function of the time difference between measurements, at the 5 regions of interest (regions a–e in Fig. 1). Only data associated with wind speeds higher than 4 m/s were used.

ACPD
10, 1983–2003, 2010

Title Page
Abstract | Introduction
Conclusions | References
Tables | Figures
◀| |▶
◀ ▶
Back | Close
Full Screen / Esc
Printer-friendly Version
Interactive Discussion

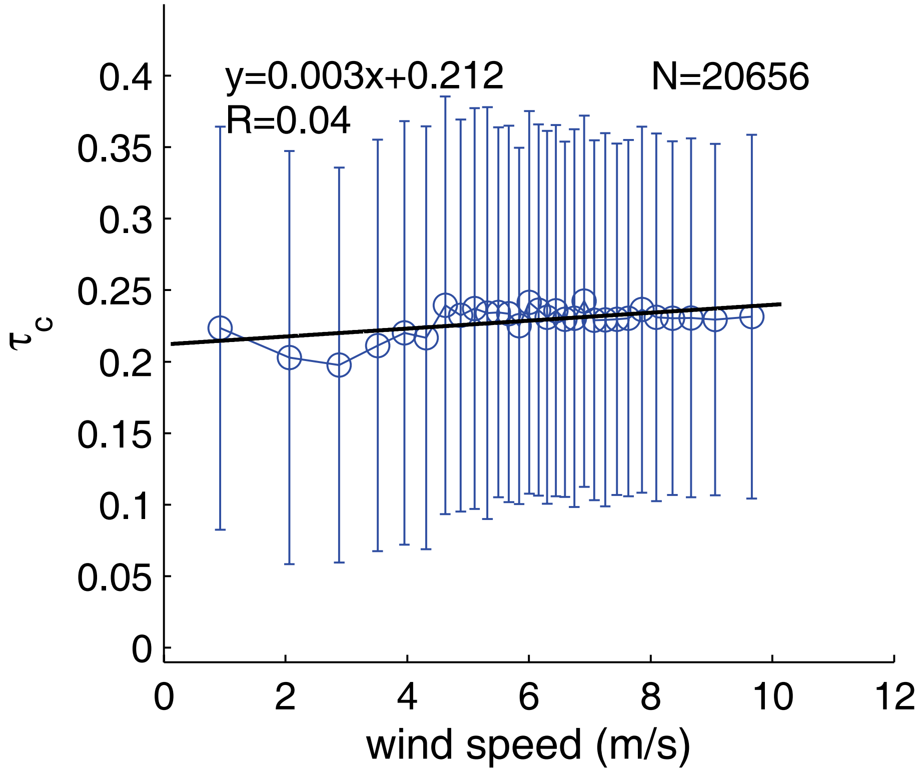

Fig. 3. MODIS τ_c plotted against QuikSCAT *W* in an area dominated by desert dust (region DD in Fig. 1a). The data were sorted according to *W* and divided into 30 bins of equal number of observations. Points and error bars represent respectively the mean and standard deviation of τ_c within each bin.

ACPD
10, 1983–2003, 2010

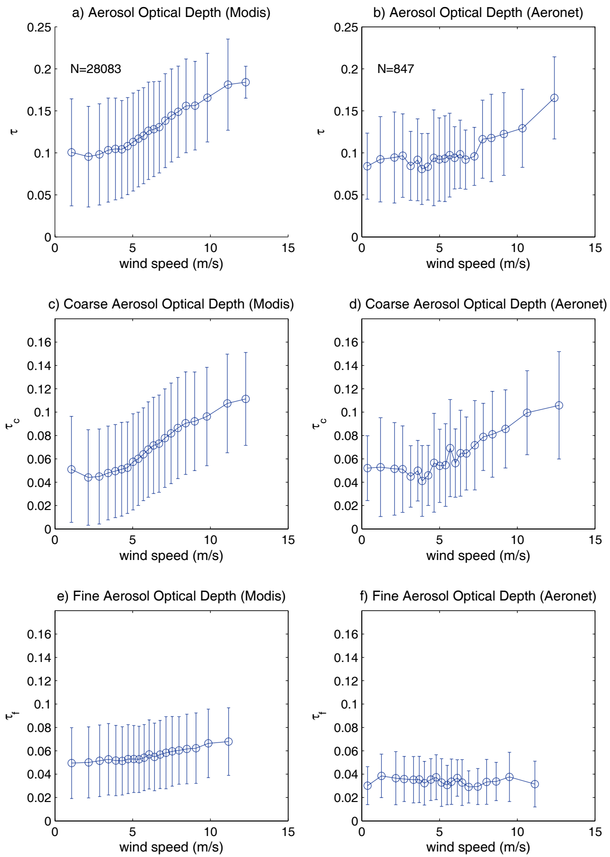

Fig. 4. AERONET (left panels) and MODIS (right panels) (**a** and **b**) τ; (**c** and **d**) τ_c; and (**e** and **f**) τ_f plotted against QuikSCAT W at Midway Island (overlapped by region a in Fig. 1). The data were sorted according to W and divided into 20 bins of equal number of observations. Circles and error bars represent respectively the mean and standard deviation of aerosol data within each bin.

ACPD
10, 1983–2003, 2010

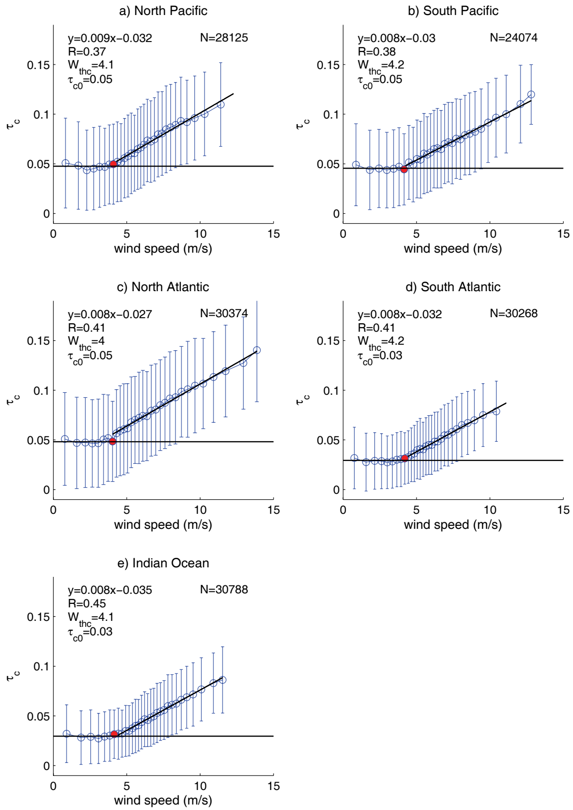

Fig. 5. MODIS τ_c plotted against QuikSCAT W at the 5 ROIs (regions a–e in Fig. 1). The data were sorted according to W and divided into 30 bins of equal number of observations. Circles and error bars represent respectively the mean and standard deviation of τ_c within each bin. The red data point and the horizontal line mark respectively the threshold wind speed for triggering coarse marine aerosol emission, W_{thc}, and the value of the background aerosol, τ_{c0} (see text). The regression equations and correlation coefficients were calculated from the full cloud of data points before binning. The statistical analysis was performed on the daily data, without spatial and temporal averaging. The regression equations and correlation coefficients were calculated for data corresponding to $W > W_{thc}$ and are shown for τ_c after subtracting the background component.

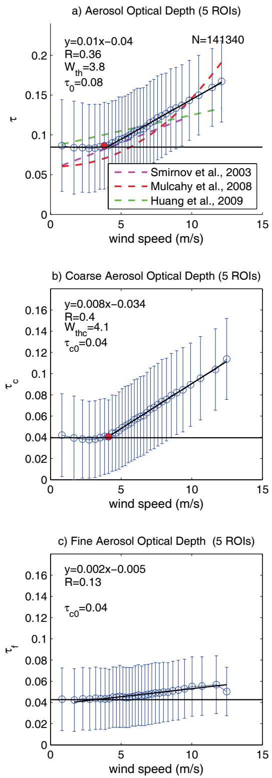

Fig. 6. MODIS **(a)** τ; **(b)** τ_c; **(c)** τ_f plotted against QuikSCAT W from the 5 regions of interest (see Fig. 1 for locations). Binning and statistical operations are similar to those in Fig. 5. The red data points in the upper and middle panels mark respectively W_{th} and W_{thc}. The horizontal black lines mark τ_0, τ_{c0} and τ_{f0} (panels a–c, respectively). The magenta, red and green dashed lines in the upper panel correspond respectively to the relationship between τ and W found by Smirnov et al. (2003), Mulcahy et al. (2008) and Huang et al. (2009).

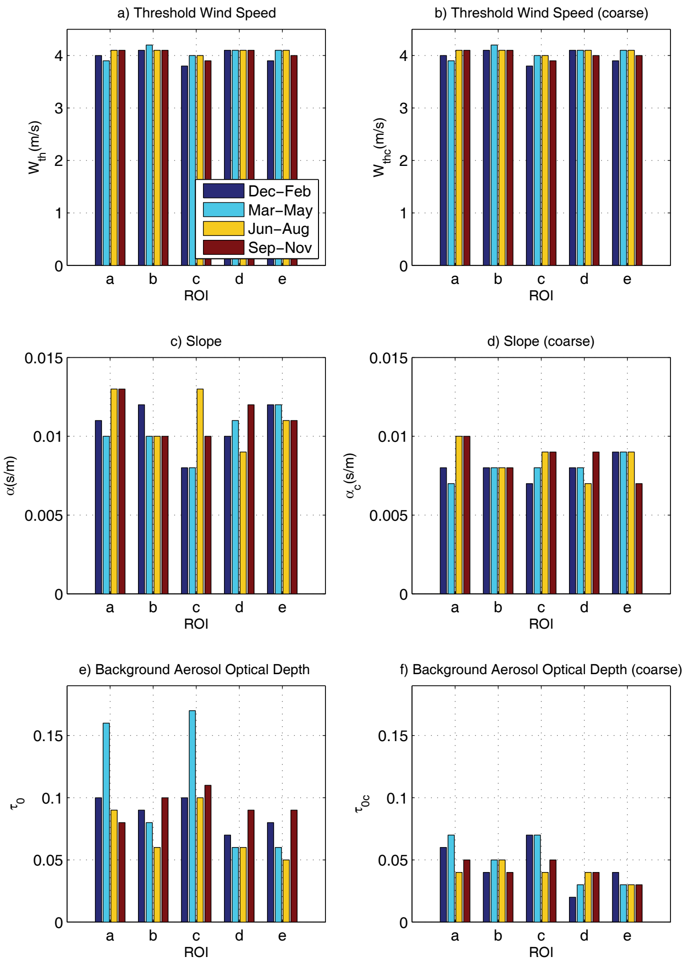

Fig. 7. Seasonal averages of **(a)** W_{th}; **(b)** W_{thc}; **(c)** α; **(d)** α_c; **(e)** τ_0; **(f)** τ_{c0}. The bars are sorted according to the regions of interest (regions a–e in Fig. 1).